THE JOURNAL OF COMPARATIVE NEUROLOGY 358:102–118 (1995)

Inositol 1,4,5-Trisphosphate Receptors: Immunocytochemical Localization in the Dorsal Cochlear Nucleus

D.K. RYUGO, T. PONGSTAPORN, D.D. WRIGHT, AND A.H. SHARP
Center for Hearing Sciences (T.P., D.K.R., D.D.W.), Departments of Otolaryngology—Head and Neck Surgery (T.P., D.K.R., D.D.W.) and Neuroscience (D.K.R., A.H.S., D.D.W.), Johns Hopkins University School of Medicine, Baltimore, Maryland 21205

ABSTRACT

In the cochlear nucleus of mammals, the relatively homogeneous responses of auditory nerve fibers are transformed into a variety of different response patterns by the different classes of resident neurons. The spectrum of these responses is hypothesized to depend on the types and distribution of receptors, ion channels, G proteins, and second messengers that form the signaling capabilities in each cell class. In the present study, we examined the immunocytochemical distribution of the inositol 1,4,5-trisphosphate (IP3) receptor in the dorsal cochlear nucleus to better understand how this second messenger might be involved in shaping the neural signals evoked by sound.

Affinity-purified polyclonal antibodies directed against the IP3 receptor labeled a homogeneous population of neurons in the dorsal cochlear nucleus of rats, guinea pigs, mustache bats, cats, New World owl monkeys, rhesus monkeys, and humans. These cells were all darkly immunostained except in the human where the labeling was less intense. Immunoblots of dorsal cochlear nucleus tissue from the rat revealed a single band of protein of molecular weight ~260 kD, which is the same size as the purified receptor, indicating that our antibodies reacted specifically with the IP3 receptor. These immunolabeled neurons were identified as cartwheel cells on the basis of shared characteristics across species, including cell body size and distribution, the presence of a highly invaginated nucleus, and a well-developed system of cisternae. Reaction product was localized along the membranes of rough and smooth endoplasmic reticulum, subsurface cisternae, and the nuclear envelope. This label was distributed throughout the cartwheel cell body and dendritic shafts but not within dendritic spines, axons, or axon terminals. The regular pattern of immunolabeling across mammals suggests that IP3 and cartwheel cells are conserved in evolution and that both play an important but as yet unknown role in hearing.

Indexing terms: auditory system, comparative neuroanatomy, electron microscopy, second messengers, synapse

The mammalian dorsal cochlear nucleus (DCN) is a key component of the auditory nervous system whose neurons are organized into a cortex (Lorente de Nó, 1981). The DCN receives direct and topographic projections from the cochlea by way of the auditory nerve (Ramón y Cajal, 1909; Fekete et al., 1984; Ryugo and May, 1993) and in turn distributes outgoing signals to higher centers (Warr, 1982). The electrophysiological responses of DCN neurons exhibit significant changes in the representation of acoustic information when compared with those of the auditory nerve (Pfeiffer, 1966; Evans and Nelson, 1973; Godfrey et al., 1975; Young et al., 1988). How specific features of sound are extracted from the environment may be embedded within these second-order response features. To understand the mechanisms that underlie this processing, there is a need to study identified cell populations, to analyze their synaptic connections, and to reveal features of their signal processing capabilities.

The diversity of neuronal responses in the cochlear nucleus has been attributed to the spatial organization of excitatory and inhibitory synapses upon the different cell types (e.g., Kiang et al., 1973; Morest et al., 1973; Tsuchitani, 1978; Cant and Morest, 1984; Banks and Sachs, 1991;

Accepted December 26, 1994.

Address reprint requests to D.K. Ryugo, Center for Hearing Sciences, Johns Hopkins University School of Medicine, 510 Traylor Research Building, 720 Rutland Avenue, Baltimore, MD 21205.

Hewitt and Meddis, 1993). The rapid excitatory responses are mediated by ligand-gated, cation-selective channels. In addition to these ionotropic receptors, however, there is at least one class of metabotropic receptors coupled to G proteins that initiate second-messenger cascades such as the inositol 1,4,5-trisphosphate (IP3; Berridge and Irvine, 1989; Ross et al., 1990; Berridge, 1993). The possibilities for information transfer within the central nervous system are expanded further by the molecular heterogeneity and regional specificities within the second-messenger phosphoinositides system (Mignery et al., 1989; Worley et al., 1989; Nakanishi et al., 1991; Peng et al., 1991; Sudhof et al., 1991; Ross et al., 1992; Berridge, 1993; Cunningham et al., 1993; Rodrigo et al., 1993, 1994; Sharp et al., 1993a,b; Suburo et al., 1993). Each neuron population presumably has a distinctive subset of receptors, G proteins, and second messengers that form part of the signaling capabilities in the cell. The spectrum of neuronal responses must therefore depend on the complement of signaling molecules present and where in the cell they are expressed.

IP3 receptor (IP3r) immunolabeling has been reported by using light microscopy for medium-sized cells in the DCN of rats (Mignery et al., 1989; Sharp et al., 1993a; Rodrigo et al., 1993, 1994). The labeled cells were proposed to be cartwheel cells, although the criteria for such an identification were not provided. The DCN contains many different populations of neurons (Lorente de Nó, 1981), and cartwheel cells represent but one of several classes of local circuit neurons. Cartwheel cells exhibit superficially located cell bodies, local circuit axons, and highly spinous apical dendrites (Lorente de Nó, 1981; Wouterlood and Mugnaini, 1984; Hackney et al., 1990; Berrebi and Mugnaini, 1991; Manis et al., 1994), but the previously identified IP3r-immunoreactive cells of the DCN did not exhibit spiny dendrites at the light microscopic level. Furthermore, the signature of cartwheel cells, subsurface cistern–mitochondrial complexes in the cell bodies (Wouterlood and Mugnaini, 1984) was not indicated. Thus, there is still some question as to the actual identity of the immunolabeled neurons reported in the DCN (Mignery et al., 1989; Sharp et al., 1993a; Rodrigo et al., 1993, 1994).

Cartwheel cells are positioned to play an important role in processing acoustic information. They are activated by the parallel fiber system of granule cells and in turn form inhibitory synapses with other local circuit and projection neurons (Berrebi and Mugnaini, 1991; Manis et al., 1994). The unambiguous identification of cartwheel cells is necessary because of their importance to central mechanisms of hearing. Consequently, we embarked on a comparative, immunocytochemical investigation of medium-sized neurons in the mammalian DCN. In the present study, we used affinity-purified polyclonal antibodies directed against the IP3 receptor and demonstrated immunocytochemically and ultrastructurally that the receptor protein is localized to a single cell type, the cartwheel cell, in a variety of mammalian species.

MATERIALS AND METHODS

Antibody production and immunoblotting

The IP3 receptor for immunization of rabbits and goats was purified from crude rat cerebellar membranes as described elsewhere (Supattapone et al., 1988; Ferris et al., 1989). Antibodies against the IP3 receptor from rat cerebellum were raised in rabbits and goats and affinity purified (Peng et al., 1991; Sharp et al., 1993a) prior to their use for immunoblotting. Total homogenates of dorsal cochlear nuclei and cerebellum were prepared from adult rats and subjected to sodium dodecyl sulfate (SDS)-polyacrylamide gel electrophoresis. The separated proteins were transferred to nitrocellulose membranes and blocked by incubation for 1 hour in 5% nonfat dry milk in phosphate buffered saline (PBS). Membranes were then incubated overnight with affinity-purified rabbit anti-IP3r antibody (AP35) at a concentration of 0.3 μg/ml, with affinity-purified goat anti-IP3r antibody (APG328) at a concentration of 0.1 μg/ml in 5% nonfat dry milk or 3% bovine serum albumin in PBS, and with anti-IP3r antibodies preadsorbed with IP3r antigen. Blots were developed by using enhanced chemiluminescence reagents (Lumiglo: Kirkegaard and Perry).

Preparation of tissue

Mustache bats (*Pteronotus parnellii*, n = 2), Sprague-Dawley rats (*Rattus norvegicus*, n = 6), pigmented guinea pigs (*Cavia porcellus*, n = 6), cats (*Felis domesticus*, n = 4), New World owl monkeys (*Aotus trivirgatus*, n = 2), and rhesus monkeys (*Macaca mulatta*, n = 6) were deeply anesthetized with sodium pentobarbital (30–50 mg/kg) and then transcardially perfused with 4% paraformaldehyde in 0.1 M phosphate buffer, pH 7.4. Tissue was then removed from the skull and further fixed in 2% paraformaldehyde in phosphate buffer for varying periods of time (1–10 days). Tissue was embedded in 5 ml of 26% (w/v) albumin and 0.5% (w/v) gelatin that was hardened with an aldehyde mixture of 1 ml stock solution of 37% formaldehyde and 0.4 ml of 5% glutaraldehyde, and then cut at a thickness of 50 μm on a Vibratome. Sections were collected and stored in 0.1 M phosphate buffer, pH 7.4, prior to processing.

Postmortem cerebellar and brainstem tissues were obtained from five humans 12–48 hours after death and placed in 4% paraformaldehyde in 0.1 M phosphate buffer, pH 7.4. Donors were of either sex and ranged from 72 to 76 years of age. There was no history of HIV or hepatitis, and there was no information on the status of their hearing. One specimen had been fixed in 1% formalin, cryoprotected, and preserved by deep freeze (−70°C) for 14 months. All human tissue was cryoprotected by being placed in a graded series of sucrose solutions (up to 30% w/v) and cut on a freezing microtome at 100-μm thickness.

Normal tissue for light microscopic analysis was mounted on slides and stained with 0.5% cresyl violet. Adjacent sections of normal and immunoprocessed tissue were prepared for combined light and electron microscopic analysis. Sections to be stained with rabbit anti-IP3r antibodies were blocked by incubation in 5% normal goat serum (NGS) in 50 mM Tris (pH 7.4) and 1.5% NaCl for 30 minutes. Sections to be stained with goat anti-IP3r antibodies were blocked with 5% normal rabbit serum (NRS) in Tris buffered saline (TBS). The sections were then incubated overnight at 4°C with gentle agitation in primary antiserum in 2% NGS (rabbit antibody) or 2% NRS (goat antibody) in TBS and 0.05% sodium azide. The affinity-purified anti-IP3r antibodies were used at a concentration of approximately 2 μg/ml. Control sections were incubated under identical conditions but without the addition of the primary antibody or by preadsorbing the antibodies with IP3 receptor antigen.

After the primary incubation, sections were rinsed and then incubated with the appropriate biotinylated secondary antibody (goat anti-rabbit or rabbit anti-goat; 1:200 dilu-

tion, Vector Laboratories) for 1 hour at room temperature. Following washes in TBS, sections were incubated with the avidin-biotin-peroxidase complex (Vector ABC Elite, Vector Laboratories) for 45 minutes, washed again with TBS, and then developed in a substrate solution containing 1 mg/ml 3,3′-diaminobenzidine (DAB) and 0.01% H_2O_2 in TBS for 10–20 minutes.

Sections of normal and immunoprocessed tissue were rinsed in TBS, placed in 1% osmium tetroxide for 15 minutes, washed 5 × 10 minutes in 0.1 M maleate buffer (pH 5.2), block stained in 2% uranyl acetate for 1 hour, dehydrated, infiltrated with Epon, and flat-embedded between two sheets of Aclar (Ted Pella, Inc.). Relevant sections were dissected and re-embedded in BEEM capsules for electron microscopic analysis. Ultrathin sections were collected on Formvar-coated slotted grids, stained with 7% uranyl acetate, and examined with a JEOL 100C electron microscope. Bat, owl monkey, and human tissue was unsatisfactory for electron microscopic analysis because the tissue was not well preserved.

Morphometric analysis

Immunostained cells from the superficial layers of the DCN of immunostained tissue and Nissl-stained cells from adjacent tissue sections of the same animals that were not subject to immunoprocessing were examined. Cells exhibiting a nucleus were drawn at a total magnification of ×2,500 (×100 oil immersion lens, NA 1.25) with the aid of a light microscope and drawing tube. Every immunostained cell in each DCN was drawn.

Cells stained by cresyl violet were selected as follows. Granule cells had small, round somata and a prominent nucleus with very little cytoplasm; these cells were primarily distributed in layer II. Pyramidal cells exhibited large cell bodies with prominent Nissl bodies and round nuclei that were lightly stained. These cells were also distributed in layer II. Medium-sized cells with round-to-oval somata and nuclei with irregular shapes, characteristic of cartwheel cells, were selected from layer I and the superficial portion of layer II. Two other known cells of the superficial DCN are Golgi and stellate cells, but they are small and difficult to distinguish at the light microscopic level. Because Golgi and stellate cells are also relatively rare (Wouterlood and Mugnaini, 1984), we do not think that they have a significant impact on this study. For each cell drawn, we determined long and short axis diameters and cross-sectional area. The greatest diameter passing through the nucleus was termed the long axis; the greatest diameter perpendicular to this long axis and passing through the nucleus was termed the short axis. Diameters and cross-sectional area of the cell bodies were determined by using a computer-aided tablet (SigmaScan, Jandel Scientific).

RESULTS

Characterization of antisera

Affinity-purified polyclonal antibodies were derived from antisera raised in one goat (APG328) and two rabbits (AP2A and AP35). APG328 and AP2A have been described elsewhere (Sharp et al., 1993a). All antisera used displayed a similar affinity for the IP3 receptor. Specificity of the rabbit and goat antisera is demonstrated in Western blots where single bands of protein, ~260,000-kD molecular weight, are stained from rat cerebellum and DCN (Fig. 1). All immunocytochemical staining produced virtually identical results when using either goat or rabbit antisera. Preadsorption of the IP3r antibodies with IP3r antigen or omission of the primary antibodies from the immunocytochemical procedure resulted in an absence of staining.

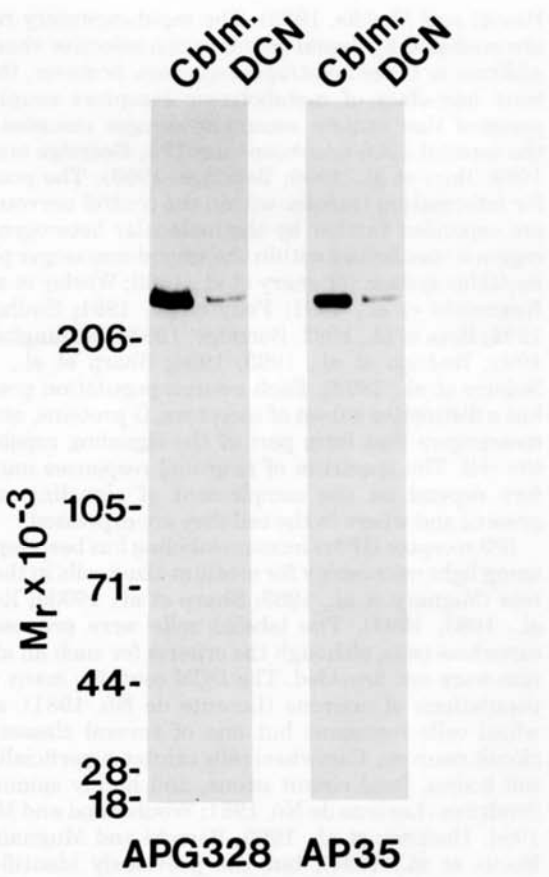

Fig. 1. Detection of inositol 1,4,5-trisphosphate receptors (IP3r) in cerebellum (Cblm.) and the dorsal cochlear nucleus (DCN) of the rat is seen by immunoblot analysis. Proteins of cerebellar and DCN homogenates were resolved by SDS-PAGE, transferred to nitrocellulose membranes, and probed with the polyclonal IP3r antibody made in goat (APG328) and rabbit (AP35). The antibodies react specifically with a single band of molecular weight ~260,000 kD. Cerebellar and DCN lanes contained 20 mg and 50 mg protein, respectively. The relative molecular masses ($M_r \times 10^{-3}$) of the standards on the gel are indicated.

IP3r immunocytochemical staining

When hindbrain tissue is immunoprocessed with the IP3r antibody, there is a characteristic staining pattern in the DCN and cerebellum (Fig. 2). A homogeneous cell population in each region is reliably and darkly immunostained. In the dorsal cochlear nucleus, a population of superficially located cells are labeled; in the cerebellar cortex, Purkinje cells are labeled.

Positive controls: IP3r immunostaining in the cerebellum

Because immunostaining with the IP3r antibody in the cerebellum was consistent and reproducible, we used the cerebellum as a positive control to evaluate our immunocytochemical procedure and to determine antibody dilution. Cerebellar Purkinje cells display high densities of the IP3 receptor not only for rats (Rodrigo et al., 1993; Sharp et al.,

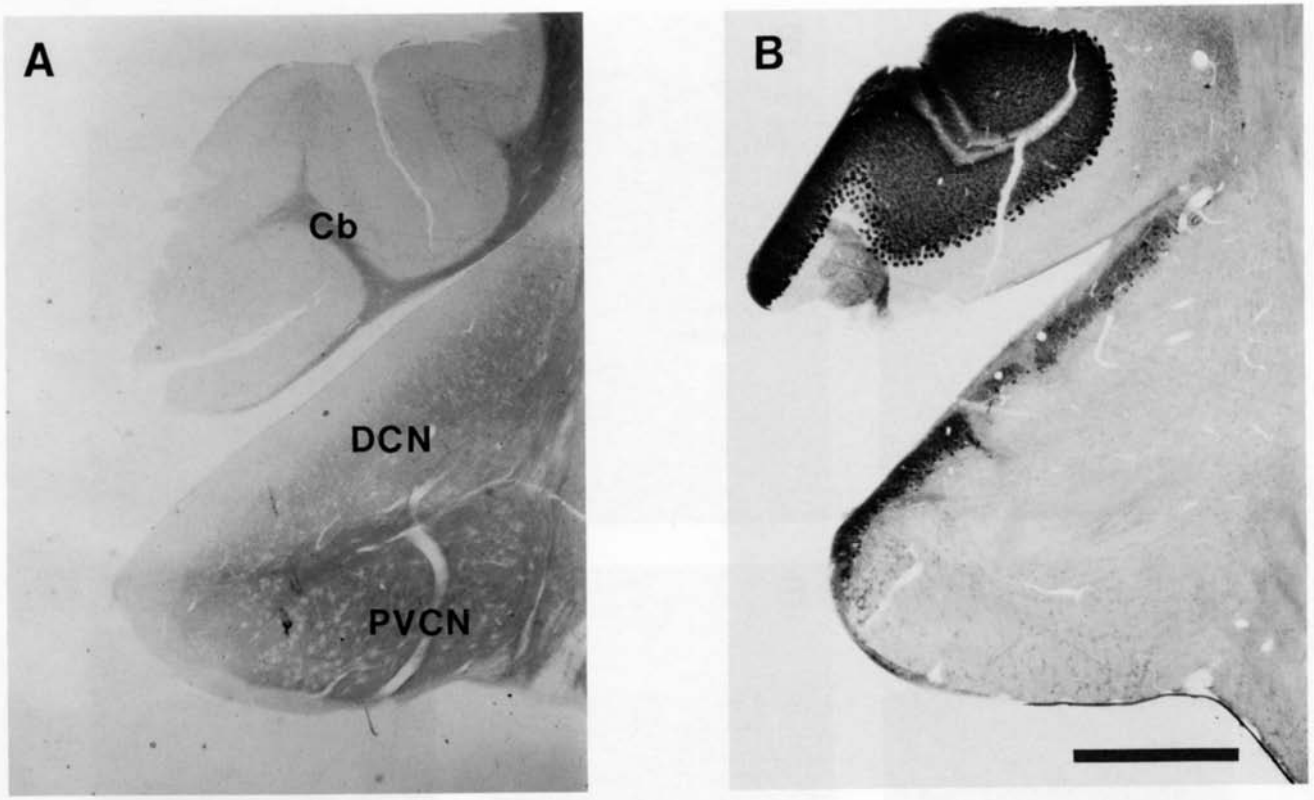

Fig. 2. Light micrographs of control (**A**) and immunostained (**B**) cat cochlear nucleus and cerebellar cortex are shown in coronal sections, using the rabbit anti-IP3r antibody. There is no tissue staining where the primary antibody is omitted in the processing (A). The background staining is the effect of osmium on white matter and our "overexposure" of the print to bring out the tissue. In contrast, the immunostained tissue (B) reveals only Purkinje cells of the cerebellum and cartwheel cells of the DCN. Lateral is to the left and dorsal is up. Cb, cerebellar cortex; DCN, dorsal cochlear nucleus; PVCN, posteroventral cochlear nucleus. Scale bar = 1 mm.

1993a,b) and human (Suburo et al., 1993) but also for guinea pigs, mustache bats, cats, owl monkeys, and rhesus monkeys (Fig. 3).

Cell bodies and dendrites are intensely stained, as are dendritic spines (Fig. 4A), recurrent collaterals (Fig. 4B) and their terminals (Fig. 4C), axons in the cerebellar white matter (Fig. 4D), and axon terminals in the deep cerebellar nuclei (e.g., dentate nucleus, Fig. 4E) and lateral vestibular nucleus (Fig. 4F). No other elements of the cerebellar cortex are stained. There are numerous punctate terminal swellings throughout the neuropil of the deep nuclei that form dense pericellular baskets around unstained cell bodies. Cerebellar Purkinje cells, including their dendrites, axons, and axon terminals, displayed identical patterns of immunoreactivity to the IP3r antibody across this variety of mammals.

IP3r immunocytochemical staining in the DCN

Immunostained neurons are distributed superficially in layers I and II (Fig. 5). There is no labeling in the deep DCN. These immunolabeled cells exhibit medium-sized cell bodies and correspond in size and shape with Nissl-stained cells having the same superficial distribution and are characterized by lightly staining cytoplasm and a lightly stained, often indented nucleus. The morphometry provides somatic size and shape data for comparisons across different mammals, not only for cartwheel cells but also for granule and pyramidal cells (Fig. 6). Although absolute cell sizes vary across different species, these quantitative data illustrate that the immunolabeled neurons maintain their relative sizes. Cells having large or small somata are not immunolabeled. The light microscopic, cytologic descriptions from Nissl material are also consistent with those published in rat and guinea pig (Wouterlood and Mugnaini, 1984; Berrebi and Mugnaini, 1991; Manis et al., 1994). The nuclei of medium-sized immunolabeled cells are round and unstained, but processes identifiable as dendrites are clearly stained (Fig. 7). Structures resembling dendritic spines were not immunostained in cells of the DCN in marked contrast to the staining of dendritic spines of Purkinje cells. In rodents, bats, and cats, immunolabeled dendrites tend to be oriented toward the pial surface, endowing the cell with a unipolar appearance (Figs. 5A,C–E, 7A,C–E). Some of these dendrites and their branches could be observed for relatively long distances (up to 150 μm in length in a 50-μm-thick tissue section) as they emerged from labeled cell bodies. Mostly, however, short segments of dendritic shafts were visible within layer I.

In primates, immunolabeled cells had somata that ranged in shape from round to polygonal and exhibited multiple dendrites that radiated away from the cell body in all

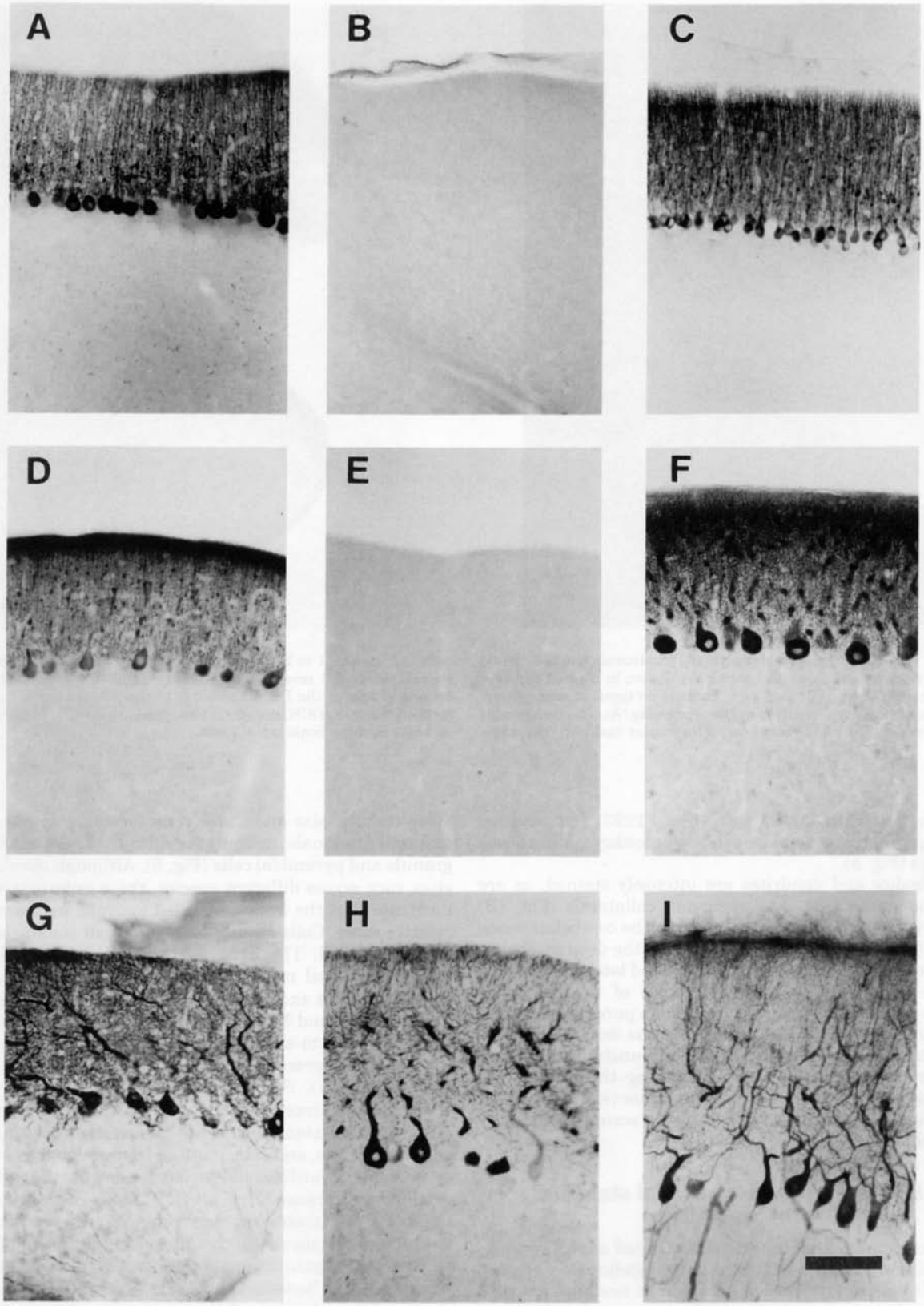

Fig. 3. Light micrographs show cerebellar cortex of different mammals, using the rabbit anti-IP3r antibody. Purkinje cells are darkly and exclusively labeled in rat (**A**), mustache bat (**C**), guinea pig (**D**), cat (**F**), owl monkey (**G**), rhesus monkey (**H**), and human (**I**). Control tissue of rat (**B**) and cat (**E**), where the primary antibody is omitted, is unstained. The pial surface is toward the top. Scale bar = 100 μm.

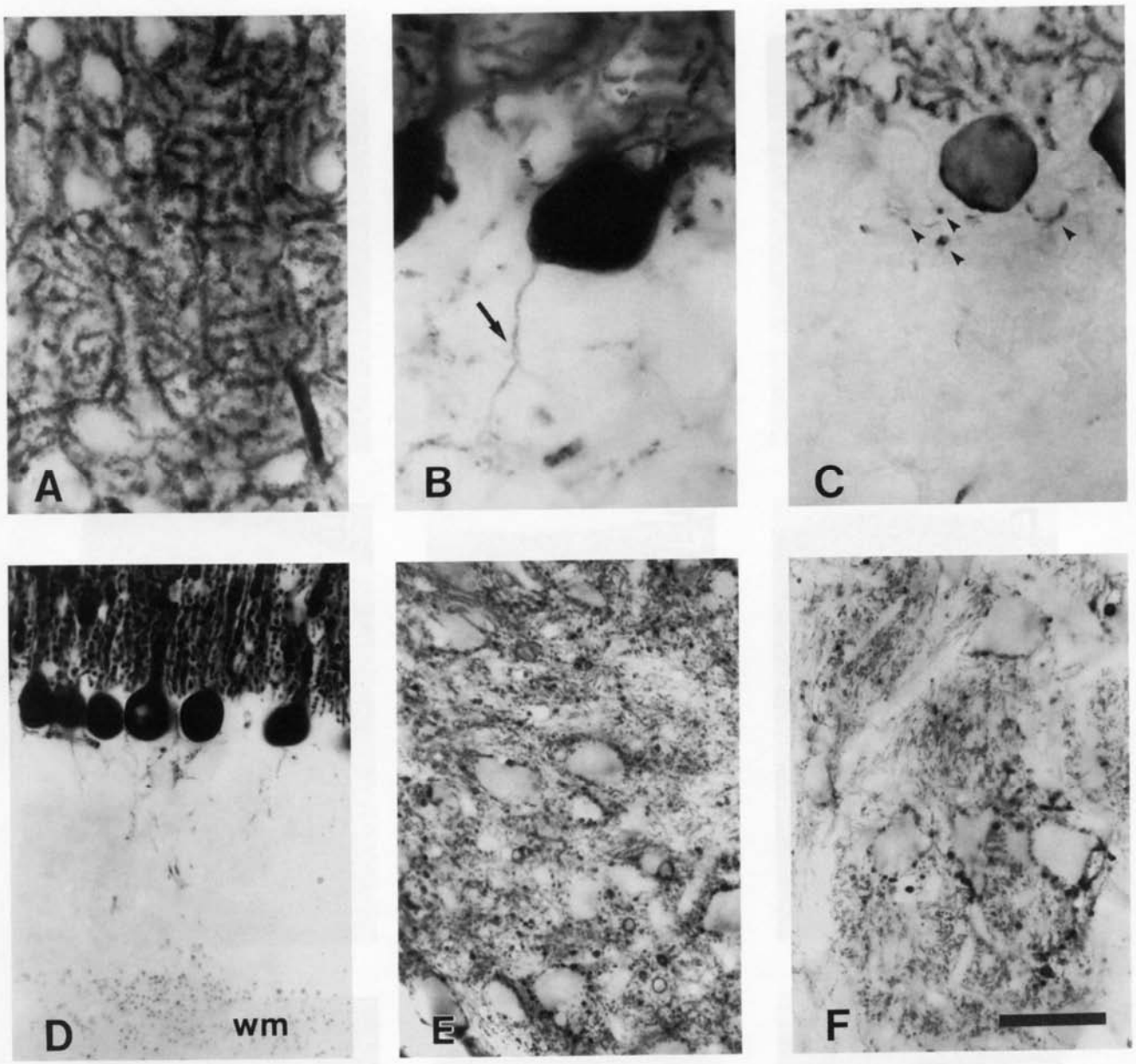

Fig. 4. Light micrographs show separate components of immunostained Purkinje cells in the rat, using the rabbit anti-IP3r antibody. There is intense labeling of dendritic shafts and dendritic spines (**A**), axon and collateral (arrow, **B**), terminals of recurrent collaterals (arrowheads, **C**), axons in the cerebellar white matter (wm, **D**), and terminals and pericellular nests in the dentate nucleus (**E**) and medial vestibular nucleus (**F**). This pattern of Purkinje cell immunostaining was similar for guinea pigs, mustache bats, cats, owl monkeys, rhesus monkeys, and human. Scale bar = 20 μm for A–C, 50 μm for D–F.

directions (Figs. 5F,G,I, 7C,D,F). These immunolabeled multipolar cells extend long, occasionally branching, dendrites that taper and resemble those of generic stellate cells. Dendritic spines were not evident at the light microscopic level (Fig. 7F,G). The distribution of these labeled cell bodies within the DCN was distinctly superficial and confined to layers I and II. It should be noted, however, that the number of the immunolabeled cells was less than that of the nonprimate mammals.

In the human DCN, immunolabeled neurons were superficially distributed but exhibited weak labeling (Fig. 5I), especially in contrast to human cerebellar Purkinje cells (Fig. 3I) and to those immunostained cells in the DCN of other mammals (Figs. 2, 5, 7). These DCN cells were nevertheless clearly stained above background and exhibited multipolar dendrites (Fig. 7I). Although the concentrations of both primary and secondary antibodies were systematically varied, human DCN cells were always more lightly labeled. This tissue was obtained from postmortem autopsy cases, and we have little information other than age and sex of the individuals. Some tissue was obtained after being frozen for 14 months; other tissue was obtained within 1–2

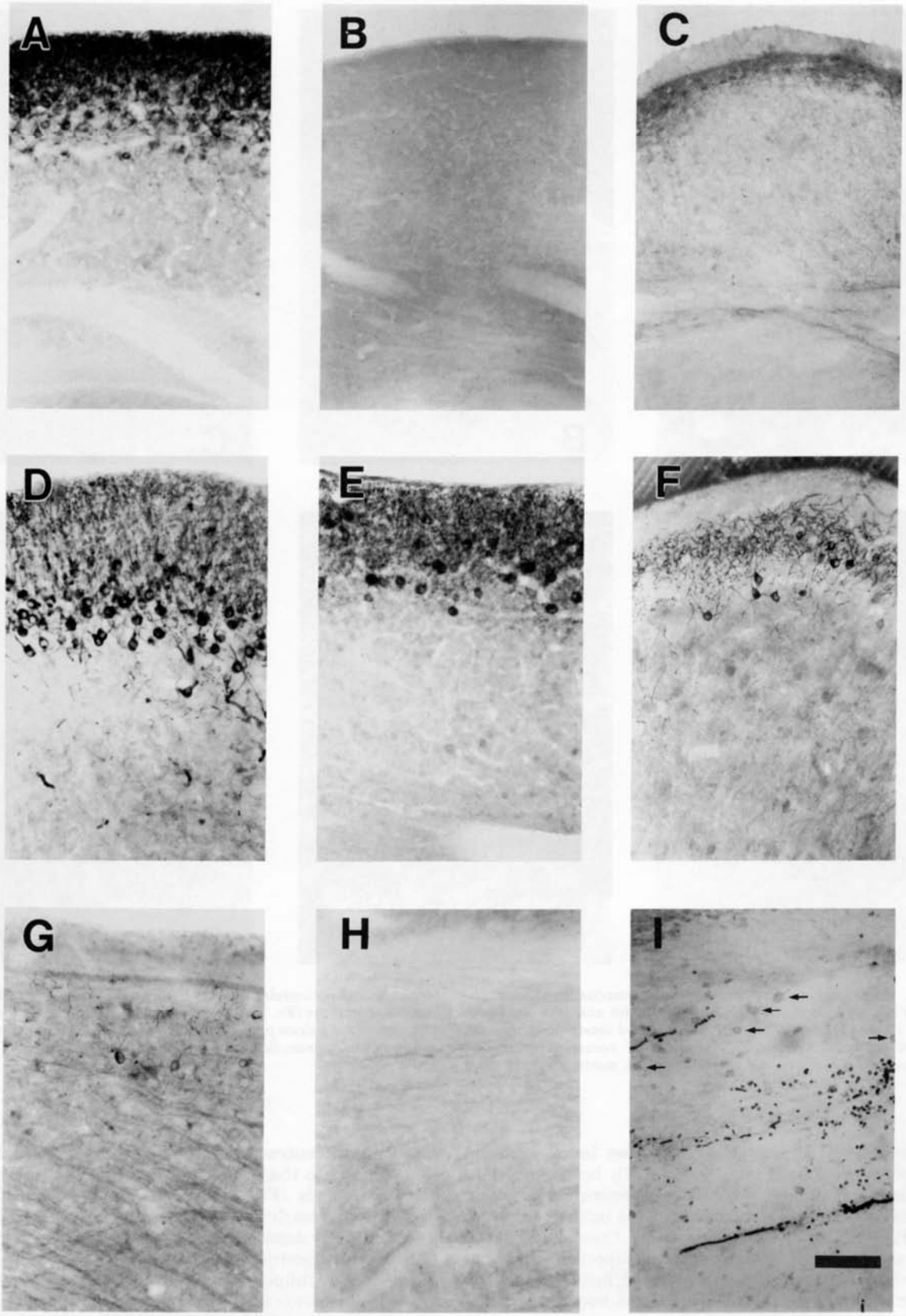

Fig. 5. Light micrographs show DCN of different mammals, using the rabbit anti-IP3r antibody. These micrographs reveal that only superficially located neurons and their dendritic processes in the nucleus are stained, as illustrated in rat (**A**), mustache bat (**C**), guinea pig (**D**), cat (**E**), owl monkey (**F**), rhesus monkey (**G**), and human (**I**). Neurons in the human DCN are less intensely stained, and some are indicated by arrows; the darkly stained, round structures are red blood cells. The pial surface is toward the top. Control tissues of rat (**B**) and rhesus monkey (**H**) are not immunostained, but lightly stained white matter is visible as a result of osmium treatment. Scale bar = 100 μm.

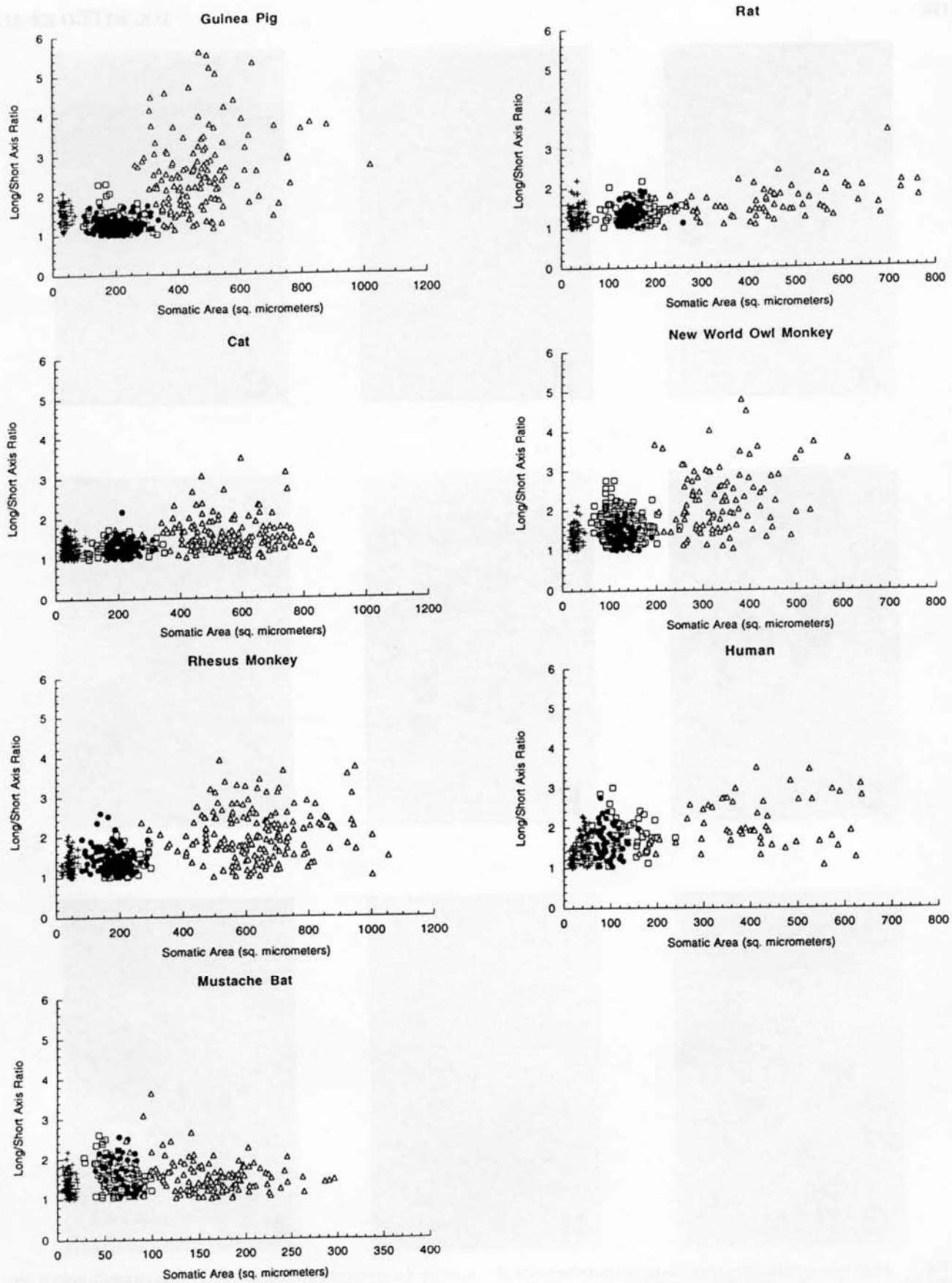

Fig. 6. Scatter plots compare size (area) and shape (axis ratio) of immunostained cells (filled circles) with Nissl-stained cells from adjacent sections in the same animals. Although the absolute size of immunostained cells is not constant (see scale changes for the X axes), their shape and relative size compared with granule cells (pluses) and pyramidal cells (open triangles) is constant. Furthermore, the morphometric features of cartwheel cells as defined in Nissl stains (open squares) closely match those of immunostained cells.

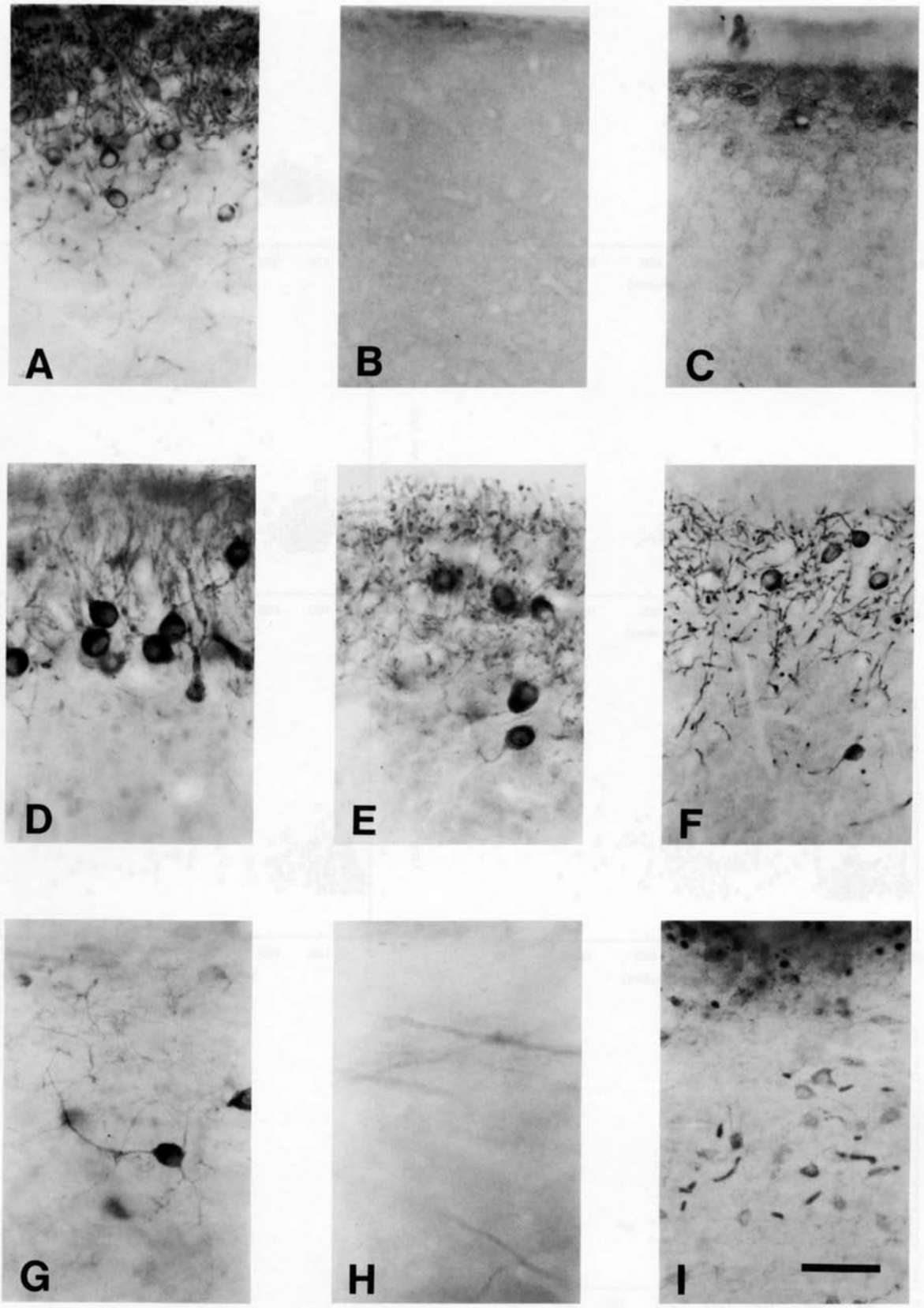

Fig. 7. Light micrographs show immunostained cartwheel cells of different mammals, using the rabbit anti-IP3r antibody. The pial surface is toward the top. In the rat (**A**), mustache bat (**C**), guinea pig (**D**), and cat (**E**), labeled dendrites have an apical orientation; in the owl monkey (**F**), rhesus monkey (**G**), and human (**I**), labeled dendrites have a multipolar arrangement. Human cells are less intensely stained, but sections with no antibody exhibited no labeling. Control tissues of rat (**B**) and rhesus monkey (**H**) are not immunostained. Axons are visible in the rhesus monkey control tissue due to osmium treatment. Scale bar = 50 μm.

Fig. 8. Electron micrograph shows a cartwheel cell in the rat DCN. Cartwheel cells for all the mammals we examined are typified by the presence of a well developed Golgi apparatus (GA) and an extensive system of cisternae (a few are indicated by arrows). Some cisternae are studded with ribosomes, whereas others associated with mitochondria are not. A subsurface cistern (arrowhead) and a mitochondrion are illustrated in close proximity to the plasma membrane; subsurface cisternal complexes are characteristic for cartwheel cells in rats but are less evident for the other mammals examined. Scale bar = 0.5 μm.

days of death. There were no obvious staining differences among the separate specimens.

Ultrastructural features of cartwheel cells

In the superficial layers of immunoprocessed control and normal DCN tissue from rats, guinea pigs, cats, and rhesus monkeys, medium-sized cell bodies (15–20 μm in diameter) are plentiful. The cytoplasm and nuclear chromatin are pale, and the nucleus is irregular in shape, typically exhibiting deep invaginations that enclose polysomes. Polysomes, rough endoplasmic reticulum (ER), and mitochondria are scattered throughout the cytoplasm. The Golgi apparatus and smooth ER are extensively developed, and cisternae characteristically appear in close spatial proximity to mitochondria (Fig. 8). A distinct organelle complex, called a subsurface cisternal complex, is found around the perimeter of the cell body, featuring a cistern squeezed between a mitochondrion and the plasma membrane (Fig. 8). In rats, these complexes are common and unambiguous markers for cartwheel cells (Wouterlood and Mugnaini, 1984), but they are less common in the species we studied (e.g., guinea pig, cat, and rhesus monkey).

Ultrastructural features of immunolabeled cells in the DCN

Immunolabeled cells of rat, guinea pig, cat, and rhesus monkey were also studied with the electron microscope. These labeled cells and their processes are characterized by the presence of electron-dense, horseradish peroxidase (HRP)-DAB reaction product, and were easily distinguishable from unlabeled cells (Fig. 9). When examined through serial sections, the nuclei of all immunolabeled cells exhibited a variable number of small, irregular pits and at least one deeply penetrating invagination (Figs. 9, 10). The reaction product is not diffuse throughout the cytoplasm

but rather seems to condense into small patches. These patches of label are scattered but accumulate in predictable sites: staining was found along the membranes of most cisternae of rough and smooth ER and subsurface cisternal complexes. This label tended to emphasize the ribosomes residing along the cisternae. The reaction product also exhibited an obvious association with the outer membrane of the nuclear envelope (Fig. 10). Reaction product was not found in association with the plasma membrane or Golgi apparatus but was occasionally observed on the external surface of mitochondria. Immunolabeled cell bodies received many bouton terminals that contained round or pleiomorphic synaptic vesicles, but cytoplasmic reaction product was not obviously associated with postsynaptic densities.

Labeled dendrites were observed to emerge exclusively and without exception from the labeled cell bodies of cartwheel cells. Unlabeled pyramidal and granule cells did not give rise to labeled dendrites. Pyramidal cells are identifiable by their large size, a clear round nucleus, and prominent stacks of rough ER that are distributed not only throughout the cell body but also within primary dendrites out to the first branch point. Granule cells are small (less than 10 μm in diameter), exhibit scant cytoplasm, and display a nucleus that is more electron dense near the envelope than in the interior. One unlabeled Golgi cell was encountered, defined by its eccentric nucleus and very irregular somatic surface (Mugnaini et al., 1980). Two unlabeled stellate cells, located just beneath the ependymal layer, were identified by their high density of cytoplasmic polyribosomes and their thin, untapered dendrites (Wouterlood et al., 1984). The definitive relationship between labeled cell bodies and labeled dendrites could be verified only when ultrathin sections included this dendrosomatic junction, and although not all dendrites could be traced back to their cell body of origin, these data indicate that the immunolabeling was specific for cartwheel cells and their dendrites.

Dendritic shafts were clearly labeled, and along these shafts were numerous dendritic spines that were distinctly unlabeled (Fig. 11). This staining motif was seen in all animals and was also consistent with the light microscopic appearance of the immunolabeled dendrites (e.g., Fig. 7). As in the cell body, the reaction product in the dendrites is amorphous and patchy, accumulating most heavily around the periphery of the shaft. Although some of the cytoplasmic detail is obscured by the reaction product, there appears to be an association of the staining with the cytoplasmic surface of smooth ER along dendritic shafts, specifically surrounding the base of dendritic spines. Sometimes, labeled smooth ER was adjacent to a patch of plasma membrane, but because such labeling appeared along the cytoplasmic side of the membrane and only occurred when the smooth ER was nearby, it did not suggest that the plasma membrane itself was labeled. The dendritic shafts received both symmetric and asymmetric synaptic contacts. There was no apparent association of reaction product with synapses along the dendritic shafts.

The dendritic spines were variable in size and shape but typically extended several micrometers from the shaft. Constrictions formed the neck of the spine, and the head of each spine was roughly 1 μm in diameter and diffusely filled with a fine, granular matrix. Sections that grazed the edge of the spine often gave the spine a dark appearance resembling label, but serial sections through the middle of such "dark" profiles revealed that the spines were in fact unlabeled. This staining variation is undoubtedly due to the curvature of the spine head. Immunolabeled dendritic shafts and their unlabeled spines were postsynaptic to en passant varicosities that arose from thin, unmyelinated axons traveling parallel to the long axis of the nucleus. The unmyelinated axons give rise to terminals filled with rounded synaptic vesicles that form asymmetric synapses with their targets. These axons fit the descriptions of parallel fibers of the cochlear granule cells. Symmetric synapses were not observed on dendritic spines.

Axons and synaptic terminals were not immunostained in the DCN. Even as axons departed from an immunolabeled cell body, they contained no immunoreaction product. The failure to detect IP3r immunostaining in axons, terminals, and dendritic spines is distinctly different from the pattern of staining in the cerebellar cortex where Purkinje cells are stained in their entirety, including somata, dendritic shafts and spines, axons, and terminals.

DISCUSSION

In the present study, we demonstrated that the inositol 1,4,5-trisphosphate receptor exhibits a reliable pattern of immunocytochemical staining in the hindbrain of mammals. Two distinct cell types are always labeled: Purkinje cells of the cerebellum and cartwheel cells of the DCN. Control experiments revealed no nonspecific staining by the antibodies. The immunocytochemical staining of brain tissue was consistent with immunoblots of rat cerebellum and DCN tissue which showed that the IP3r antibody reacted with a single band of protein, molecular weight ~260 kD, which is the same size as the purified receptor (Supattapone et al., 1988; Furuichi et al., 1989; Mignery et al., 1989, 1990; Maeda et al., 1990). The observations for rodents, bats, cats, and primates were similar when using goat and rabbit antibodies made against rat IP3 receptors, suggesting that the same molecule is being recognized in all cases. These data imply that IP3 is conserved in Purkinje and cartwheel cells across mammals.

Comparative analysis of cartwheel cells

Cartwheel cells have been described in the literature, by using different staining methods, studying different species at different ages, and applying different morphologic criteria (Brawer et al., 1974; Lorente de Nó, 1981; Wouterlood and Mugnaini, 1984; Hackney et al., 1990; Manis et al., 1994). They have been most thoroughly studied in rats and guinea pigs, where they exhibit medium-sized (15–20 μm in diameter) cell bodies that are round-to-oval in shape and distributed primarily in layers I and II of the DCN. Each cell body gives rise to 3–5 primary dendrites that extend apically into layer I, branch relatively infrequently, and are laden with spines. The round nucleus is centrally placed, stains lightly with basic dyes, and exhibits one or several deep invaginations. At the ultrastructural level, cartwheel cells contain subsurface cisternal complexes.

Our observations that there are both similarities and differences in the morphologic appearance of immunolabeled cells of the DCN in different species make unambiguous identification of neuron types (e.g., cartwheel cells) difficult. One problem is determining which features unify the class of neurons, which ones simply reflect variations on

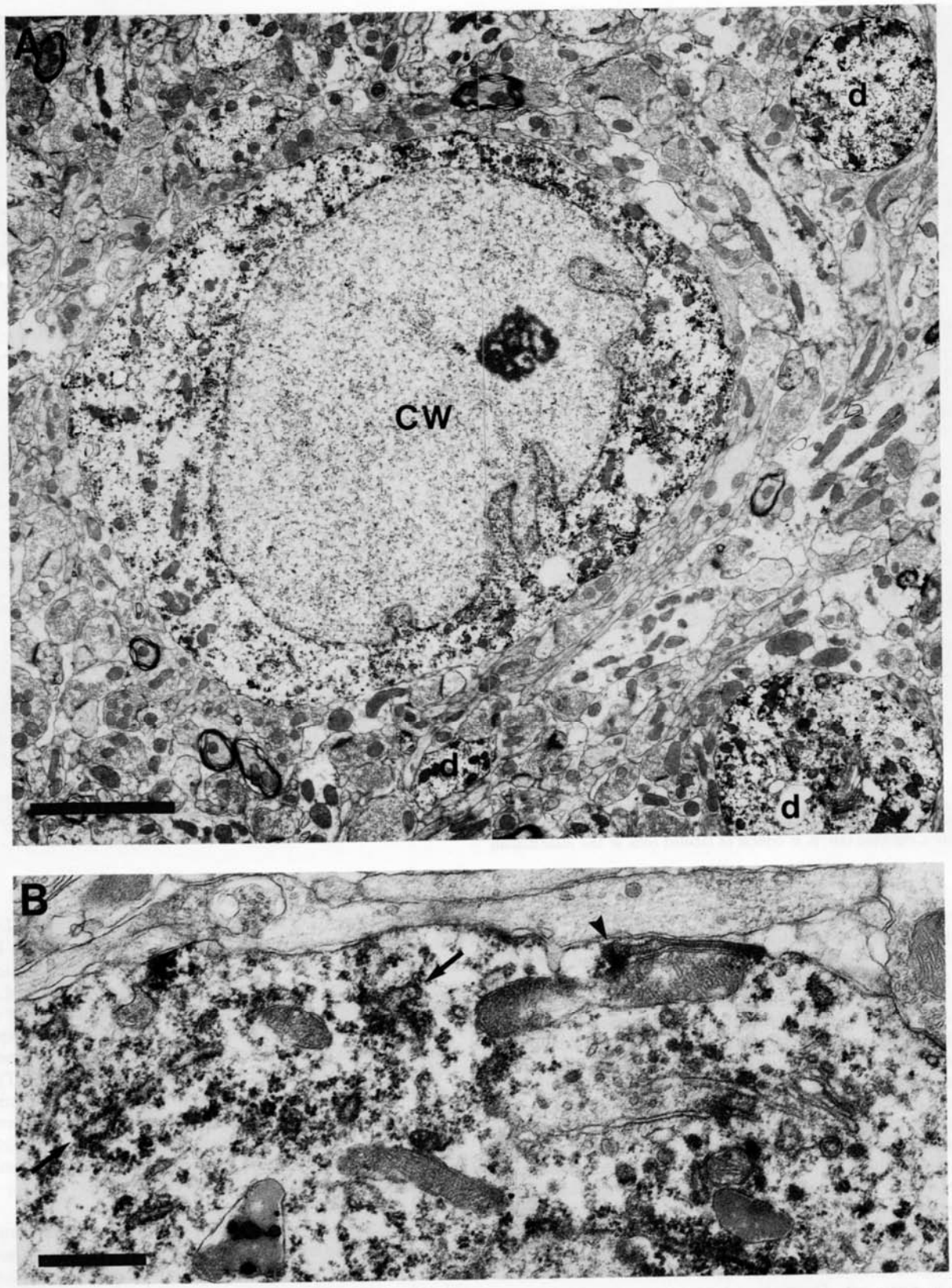

Fig. 9. **A:** Low-magnification electron micrograph shows immunolabeled cartwheel cell (CW) in the rat DCN. The immunoperoxidase reaction product appears as black precipitate that is associated with the cisternae of rough and smooth endoplasmic reticulum (ER), subsurface cisternae, and the outer leaflet of the nuclear envelope. The labeled cell exhibits a highly infolded nuclear membrane that is characteristic of the class of cartwheel cells. Immunolabeled dendritic shafts (d) are also evident in the neuropil. **B:** Higher magnification electron micrograph through cartwheel cell illustrates black reaction product along cytoplasmic cisternae (arrows) and a subsurface cistern (arrowhead), using rabbit anti-IP3r antibody. Scale bars = 3 μm in A, 0.5 μm in B.

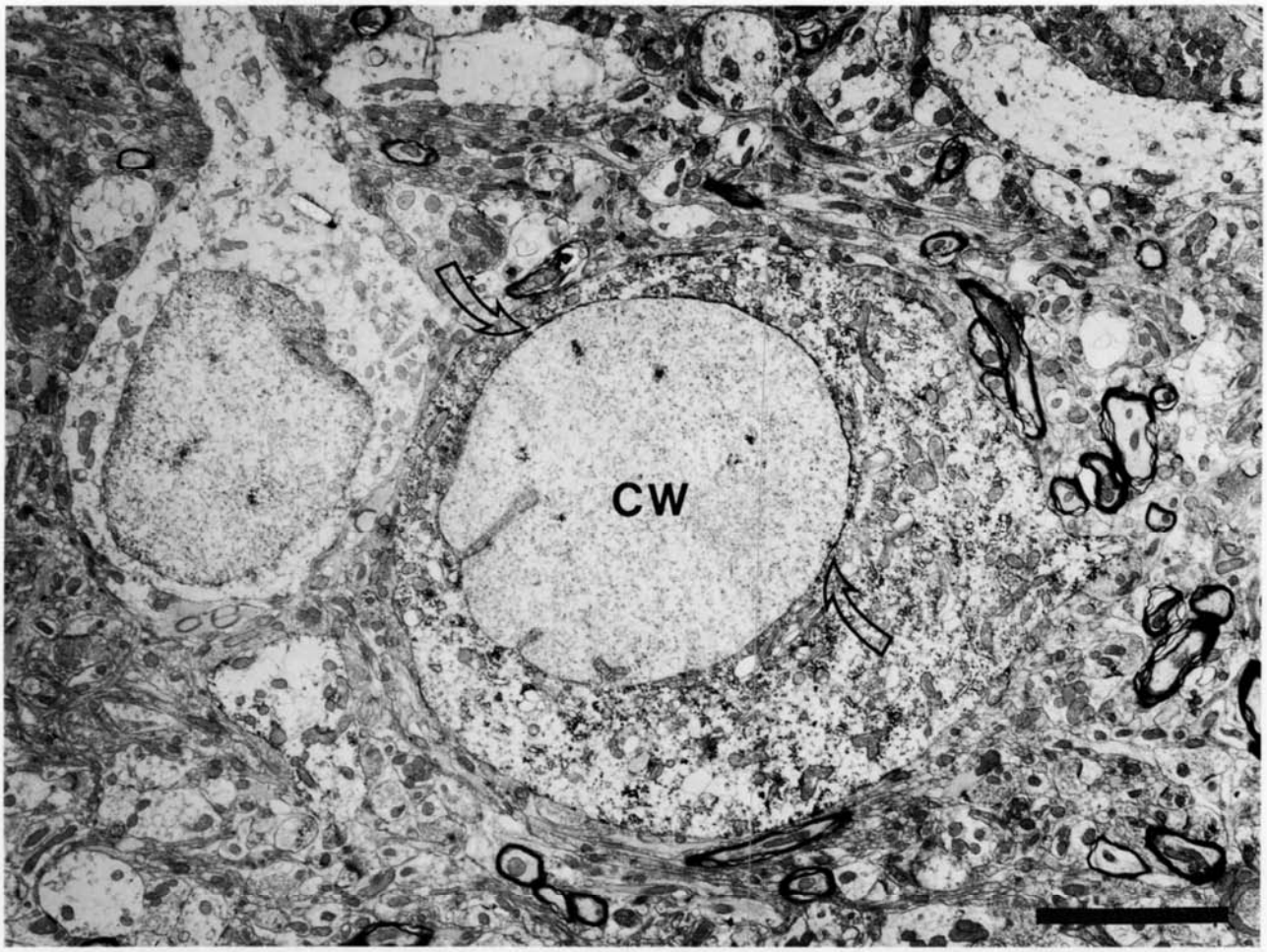

Fig. 10. Electron micrograph shows immunolabeled cartwheel cell (CW) in the DCN of rhesus monkey, using the rabbit anti-IP3r antibody. This immunolabeled cell is easily distinguished from the adjacent unlabeled cell. It is typical of labeled cells in the mammalian DCN to exhibit an infolded nucleus and immunoprecipitate along the nuclear membrane (between arrows) and cytoplasmic cisternae. Scale bar = 5 μm.

a theme, and which ones represent an entirely new theme. Immunolabeled cells of the DCN contain the IP3 receptor, have medium-sized cell bodies with a superficial distribution, and exhibit a high density of dendritic spines. Furthermore, the IP3 receptor distribution is subcellularly localized within cisternae and the nuclear envelope, and there is no labeling in dendritic spines, yet there is dense labeling in dendritic shafts in all mammalian species studied. Finally, the dendritic shafts and spines of cartwheel cells are postsynaptic to en passant terminals of parallel fibers. The specificity of IP3 receptor immunolabeling in the DCN and the consistent morphologic features of immunolabeled medium-sized cells across species lead us to conclude that these cells are cartwheel cells and that they represent a key component to central mechanisms in mammalian hearing.

In the mammals we examined, cell bodies and dendritic shafts of cartwheel cells were strongly immunolabeled with IP3r antibodies but dendritic spines, axons, and synaptic endings were not. Dendritic spines are prominent structural features of cartwheel cells in rats, guinea pigs, and cats (Brawer et al., 1974; Wouterlood and Mugnaini, 1984; Manis et al., 1994). We have resolved one inconsistency in the descriptions of IP3r immunolabeled cells in the DCN. Although IP3r labeled cells appear nonspiny at the light microscopic level, we demonstrated with electron microscopy that dendritic shafts are strongly immunostained, but dendritic spines, although present and plentiful, are not. The distribution of IP3 receptors in different compartments of individual neurons emphasizes the importance of local effects for the fine control of neuronal function. These data also stand partially opposed to the idea that the human DCN has a unique neuronal organization among mammals (Moore and Osen, 1979; Adams, 1986). The conservation of this immunocytochemical feature across mammalian orders suggests a significant but as yet unknown role for this second messenger in hearing.

There was some variability in the number of immunolabeled cells in the mammalian DCN. It seemed that the bat and primate had fewer cartwheel cells than nonprimates. In primates, this reduction in cartwheel cell number may be related to an observation that cochlear granule cells in primates exhibit a similar reduction (Moore, 1980). Cartwheel and granule cell populations, both of which partici-

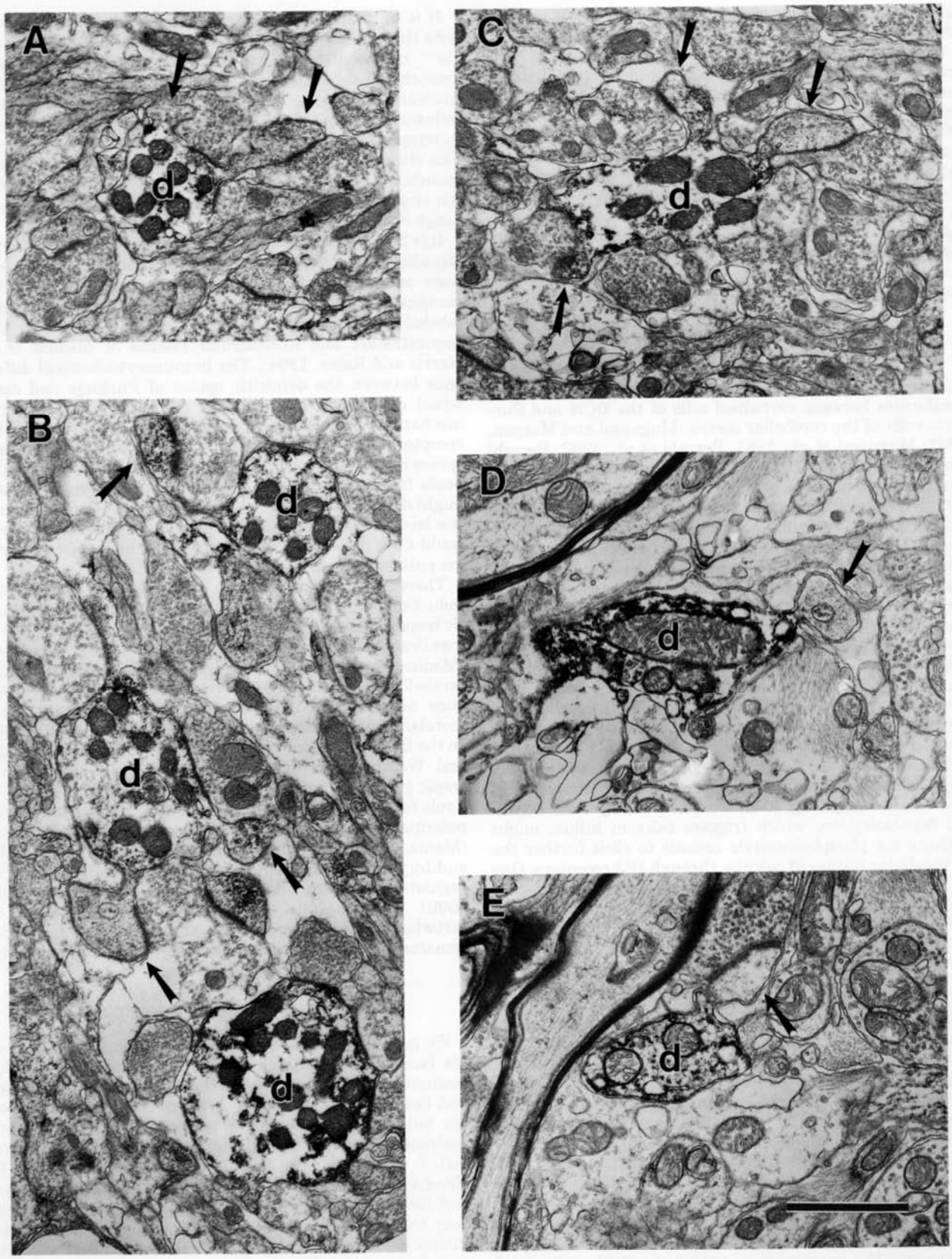

Fig. 11. Electron micrographs show neuropil in the molecular layer of the DCN. These micrographs illustrate immunolabeled dendritic shafts (d) of cartwheel cells giving rise to unlabeled dendritic spines (arrows) of rat (**A**), guinea pig (**B**), cat (**C**), and rhesus monkey (**D,E**). Cartwheel cell dendritic shafts and spines are postsynaptic to terminals containing round vesicles that originate from parallel fibers. Rabbit anti-IP3r antibody was used for A–D; goat anti-IP3r antibody was used for E. Scale bar = 1 μm.

pate in the same neural circuit (Wouterlood and Mugnaini, 1984), may share similar phylogenetic fates.

The cortical organization of the DCN is apparent in Nissl preparations of most mammals but is often more difficult to detect in primates (Moore, 1980). IP3r immunocytochemistry, however, reveals a clear laminar organization for the DCN of the mammals we examined, including humans, again emphasizing a fundamental plan for DCN structure. Primate cartwheel cells exhibit multipolar dendrites rather than unipolar ones, a feature that contributes to differences in the DCN molecular layer between primates and nonprimates and to the diminution of a well-defined molecular layer. Exactly how the dendritic polarity of cartwheel cells influences signal processing in the nucleus remains to be answered.

Comparisons between cartwheel and Purkinje cells

There is a great deal of literature that compares the similarities between cartwheel cells of the DCN and Purkinje cells of the cerebellar cortex (Mugnaini and Morgan, 1987; Mugnaini et al., 1987; Berrebi et al., 1990; Berrebi and Mugnaini, 1991). We have demonstrated, however, that these two cell populations do exhibit immunocytochemical differences with respect to IP3 receptors: the dendritic spines and axon terminals of Purkinje cells are intensely immunolabeled, whereas those of cartwheel cells are not. The significance of IP3 receptors in dendritic spines of Purkinje cells but not in the spines of cartwheel cells is unknown, but this difference presumably reflects some key variation in the mechanism of intracellular signaling. It also raises questions about how IP3 and calcium function during synaptic transmission in these separate cell populations. Cartwheel and Purkinje cells may require different strategies to handle coincident activity that underlie "synaptic learning" because cartwheel cells do not receive climbing fiber inputs.

The difference in distribution of IP3 receptors in axon terminals implies a further difference in mechanisms of intercellular signaling. In the case of Purkinje cells, terminal depolarization, which triggers calcium influx, might activate the phosphoinositide cascade to elicit further the intracellular release of calcium through IP3 receptors. One implication is that Purkinje cells but not cartwheel cells exert local influences over their synaptic terminals by way of this second-messenger system.

Significance of IP3 receptors in cartwheel cell signaling

Cartwheel cells discharge complex action potentials in response to depolarizing current that appear to be mediated by Ca^{++} (Hirsch and Oertel, 1988; Zhang and Oertel, 1993; Manis et al., 1994). Each action potential consists of an initial fast spike followed within 10 ms by one or more smaller spikes riding on a slow depolarization wave. Typically, these bursts appear in all-or-none fashion, occurring as either spontaneous or evoked discharges. They arise from fast depolarizing postsynaptic potentials (EPSPs) and resemble the Ca^{++} spikes of the cerebellum (Llinas and Sugimori, 1980; Manis et al., 1994). These complex action potentials of cartwheel cells occur too quickly to be mediated by the IP3 sensitive Ca^{++} pools but could be influenced by this second-messenger cascade with repetitive stimulation. More information is clearly needed on this topic.

It is of interest that IP3r immunolabeling is associated with the membranes of cisternae and the nuclear envelope. Ca^{++} may well be stored in the cisternae of rough and smooth ER, subsurface cisternae, and in the space between nuclear membranes. The mobilization of intracellular Ca^{++} following the binding of IP3 to its receptor is hypothesized to trigger any of a number of calcium-dependent reactions. The close proximity of subsurface cisternae to the plasma membrane may facilitate activation of calcium-regulated ion channels because of the limited intracellular diffusion range of Ca^{++} (Allbritton et al., 1992).

It is highly probable that calcium plays a major role in the signaling properties of cartwheel cells. The IP3 receptor has been revealed as both the Ca^{++} channel and the IP3 recognition site (Ferris et al., 1989). Smooth ER is immunolabeled in cartwheel cells and may be involved in the sequestration and intracellular release of calcium (e.g., Harris and Kater, 1994). The immunocytochemical difference between the dendritic spines of Purkinje and cartwheel cells is an indication of the diversity of possible mechanisms for intracellular signaling. The presence of IP3 receptors in the dendritic shafts of cartwheel cells but not spines may be a mechanism that isolates the different Ca^{++} pools from one another. The pattern of synaptic inputs might determine which Ca^{++} pools are mobilized, such that the level of Ca^{++} in the particular neuronal compartment could then determine which enzymatic or second-messenger pathway is initiated.

There is abundant evidence for a role of calcium in the induction of long-term alterations in the strength of synaptic transmission. This kind of plasticity at a cellular level is manifest by long-term potentiation in the hippocampus (Madison et al., 1991) and long-term depression in the cerebellum (Linden, 1994) and seems to involve the presence of N-methyl-D-aspartate (NMDA) receptors and metabotropic glutamate receptors (Nakanishi, 1992, 1994). In the DCN, cartwheel cells have NMDA receptors (Petralia and Wenthold, unpublished observations) and metabotropic glutamate receptors (Wright et al., 1993), indicating a role for these cells in synaptic plasticity. The possibility of potentiation involving part of the cartwheel cell circuit (Manis, 1989) may indicate that cellular plasticity in the auditory system has a behavioral expression, such as in regulating the acoustic startle response (Boulis et al., 1990). How phosphoinositol cascades serve the role of cartwheel cells in modulating the output of the DCN remains an important issue that has yet to be determined.

ACKNOWLEDGMENTS

We gratefully thank S.H. Snyder for support and use of his facilities, P.B. Manis and D.L. Weedman for helpful discussions of the data, and Melanie Carr, Sussan Paydar, and Denise Vause for technical assistance. We also thank the following individuals for helping to provide us with brainstem tissue: Dr. G.D. Pollak for bats, Drs. A. Morel and J. Kaas for New World owl monkeys, Drs. S.H.C. Hendry, M.A. Steinmetz, and D.S. Zee for rhesus monkeys, and Dr. L.J. Martin for one human specimen. The other four human brains were obtained through the Maryland Anatomy Board, University of Maryland School of Medicine, Baltimore. Portions of this work were presented at the annual midwinter meeting of the Association for Research in Otolaryngology in February 1992. This work was sup-

ported by NIH grants DC00232 and DC00979, and the W.M. Keck Foundation.

LITERATURE CITED

Adams J.C. (1986) Neuronal morphology in the human cochlear nucleus. Arch. Otolaryngol. Head Neck Surg. *112:*1253–1261.

Allbritton, N.L., T. Meyer, and L. Stryer (1992) Range of messenger action of calcium ion and inositol 1,4,5-trisphosphate. Science *258:*1812–1815.

Banks, M.I., and M.B. Sachs (1991) Regularity analysis in a compartmental model of chopper units in the anteroventral cochlear nucleus. J. Neurophysiol. *65:*606–629.

Berrebi, A.S., and E. Mugnaini (1991) Distribution and targets of the cartwheel cell axon in the dorsal cochlear nucleus of the guinea pig. Anat. Embryol. *183:*427–454.

Berrebi, A.S., J.I. Morgan, and E. Mugnaini (1990) The Purkinje cell class may extend beyond the cerebellum. J. Neurocytol. *19:*643–654.

Berridge, M.J. (1993) Inositol trisphosphate and calcium signalling. Nature *361:*315–325.

Berridge, M.J., and R.F. Irvine (1989) Inositol phosphates and cell signalling. Nature *341:*197–205.

Boulis, N.M., J.H. Kehne, M.J.D. Miserendino, and M. Davis (1990) Differential blockade of early and late components of acoustic startle following intrathecal infusion of 6-cyano-7-nitroquinoxaline-2,3-dione (CNQX) or D,L-2-amino-5-phosphonovaleric acid (AP-5). Brain Res. *520:*240–246.

Brawer, J.R., D.K. Morest, and E.C. Kane (1974) The neuronal architecture of the cochlear nucleus of the cat. J. Comp. Neurol. *155:*251–300.

Cant, N.B., and D.K. Morest (1984) The structural basis for stimulus coding in the cochlear nucleus of the cat. In C.I. Berlin (ed): Hearing Science: Recent Advances. San Diego: College Park Press, pp. 371–421.

Cunningham, A.M., D.K. Ryugo, A.H. Sharp, R.R. Reed, S.H. Snyder, and G.V. Ronnett (1993) Neuronal inositol 1,4,5-trisphosphate receptor localized to the plasma membrane of olfactory cilia. Neuroscience *57:*339–352.

Evans, E.F., and P.G. Nelson (1973) The responses of single neurones in the cochlear nucles of the cat as a function of their location and anesthetic state. Exp. Brain Res. *17:*402–427.

Fekete, D.M., E.M. Rouiller, M.C. Liberman, and D.K. Ryugo (1984) The central projections of intracellularly labeled auditory nerve fibers in cats. J. Comp. Neurol. *22:*432–450.

Ferris, C.D., R.L. Huganir, S. Supattapone, and S.H. Snyder (1989) Purified inositol 1,4,5-trisphosphate receptor mediates calcium influx in reconstituted lipid vesicles. Nature *342:*87–89.

Furuichi, T., S. Yoshikowa, A. Miyawaki, K. Wada, N. Maeda, and K. Kikoshiba (1989) Primary structure and functional expression of the inositol 1,4,5-trisphosphate-binding protein P400. Nature *342:*32–38

Godfrey, D.A., N.Y-S. Kiang, and B.E. Norris (1975) Single unit activity in the dorsal cochlear nucleus of the cat. J. Comp. Neurol. *162:*269–284.

Hackney, C.M., K.K. Osen, and J. Kolston (1990) Anatomy of the cochlear nuclear complex of guinea pig. Anat. Embryol. *182:*123–149.

Harris, K.M., and S.B. Kater (1994) Dendritic spines: Cellular specializations imparting both stability and flexibility to synaptic function. Ann. Rev. Neurosci. *17:*341–371.

Hewitt, M.J., and R. Meddis (1993) Regularity of cochlear nucleus stellate cells: A computational modeling study. J. Acoust. Soc. Am. *93:*3390–3399.

Hirsch, J.A., and D. Oertel (1988) Intrinsic properties of neurones in the dorsal cochlear nucleus of mice, in vitro. J. Physiol. *396:*535–548.

Kiang, N.Y-S., D.K. Morest, D.A. Godfrey, J.J. Guinan, Jr., and E.C. Kane (1973) Stimulus coding at caudal levels of the cat's auditory nervous system. I. Response characteristics of single units. In A.R. Moller (ed): Basic Mechanisms of Hearing. New York: Academic Press, pp. 455–478.

Linden, D.J. (1994) Long-term synaptic depression in the mammalian brain. Neuron *12:*457–472.

Llinas, R., and M. Sugimori (1980) Electrophysiological properties of in vitro Purkinje cell somata in mammalian cerebellar slices. J. Physiol. *305:*171–195.

Lorente de Nó, R. (1981) The Primary Cochlear Nuclei. New York: Raven Press.

Madison, D.M., R.C. Malenka, and R.A. Nicoll (1991) Mechanisms underlying long-term potentialtion of synaptic transmission. Ann. Rev. Neurosci. *14:*379–397.

Maeda, N., M. Niinobe, and K. Mikoshiba (1990) A cerebellar Purkinje cell marker P_{400} protein is an inositol 1,4,5-trisphosphate ($InsP_3$) receptor protein. Purification and characterization of $InsP_3$ receptor complex. Eur. Mol. Biol. Org. J. *9:*61–67.

Manis, P.B. (1989) Responses to parallel fiber stimulation in the guinea pig dorsal cochlear nucleus in vitro. J. Neurophysiol. *61:*149–161.

Manis, P.B., G.A. Spirou, D.D. Wright, S. Paydar, and D.K. Ryugo (1994) Physiology and morphology of complex spiking neurons in the guinea pig dorsal cochlear nucleus. J. Comp. Neurol. *348:*261–276.

Mignery, G.A., T.C. Sudhof, K. Takei, and P. De Camilli (1989) Putative receptor for inositol 1,4,5-triphosphate similar to ryanodine receptor. Nature, *342:*192–195.

Mignery, G.A., C.L. Newton, B.T. Archer III, and T.C. Sudhof (1990) Structure and expression of the rat inositol 1,4,5-triphosphate receptor. J. Biol. Chem. *265:*12679–12685.

Moore, J.K. (1980) The primate cochlear nuclei: Loss of lamination as a phylogenetic process. J. Comp. Neurol. *193:*609–129.

Moore, J.K., and K.K. Osen (1979) The cochlear nuclei in man. Am. J. Anat. *154:*393–418.

Morest, D.K., N.Y-S. Kiang, E.C. Kane, J.J. Guinan, Jr., and D.A. Godfrey (1973) Stimulus coding at caudal levels of the cat's auditory nervous system. II. Pattern of synaptic organization. In A.R. Moller (ed): Basic Mechanisms of Hearing. New York: Academic Press, pp. 479–504.

Mugnaini E., and J.I. Morgan (1987) The neuropeptide cerebellin is a marker for two similar neuronal circuits in rat brain. Proc. Natl. Acad. Sci. USA *84:*8692–8696.

Mugnaini, E., K.K. Osen, A.-L. Dahl, V.L. Friedrich, and G. Korte (1980) Fine structure of granule cells and related interneurons (termed Golgi cells) in the cochlear complex of cat, rat and mouse. J. Neurocytol. *9:*537–570.

Mugnaini, E., A.S. Berrebi, A-L. Dahl, and J.I. Morgan (1987) The polypeptide PEP-19 is a marker for Purkinje neurons in cerebellar cortex and cartwheel neurons in dorsal cochlear nucleus. Arch. Ital. Biol. *126:*41–67.

Nakanishi, S. (1992) Molecular diversity of glutamate receptors and implications for brain function. Science *258:*597–603.

Nakanishi, S. (1994) Metabotropic glutamate receptors: Synaptic transmission, modulation, and plasticity. Neuron *13:*1031–1037.

Nakanishi, S., N. Maeda, and K. Mikoshiba (1991) Immunohistochemical localization of an inositol 1,4,5-trsiphosphate receptor, P_{400} in neural tissue: Studies in developing and adult mouse brain. J. Neurosci. *11:*2075–2086.

Peng, Y.-W., A.H. Sharp, S.H. Synder, and K.-W. Yau (1991) Localization of the inositol 1,4,5-trisphosphate receptor in synaptic terminals in the vertebrate retina. Neuron *6:*525–531.

Pfeiffer, R.R. (1966) Classification of response patterns of spike discharges for units in the cochlear nucleus: Tone burst stimulation. Exp. Brain Res. *1:*220–235.

Ramón y Cajal, S. (1909) Histologie du Système nerveux de l'Homme et des Vertébrés, vol 1 (reprint 1952). Madrid: Instituto Ramón y Cajal, pp. 774–838.

Rodrigo, J., A.M. Suburo, M.L. Bentura, T. Fernández, S. Nakade, K. Mikoshiba, R. Martínez-Murillo, and J.M. Polak (1993) Distribution of the inositol 1,4,5-trisphosphate receptor, P400, in adult rat brain. J. Comp. Neurol. *337:*493–517.

Rodrigo, J., O. Uttenthal, M.L. Bentura, N. Maeda, K. Mikoshiba, R. Martínez-Murillo, and J.M. Polak (1994) Subcellular localization of the inositol 1,4,5-trisphosphate receptor, P400, in the vestibular complex and dorsal cochlear nucleus of the rat. Brain Res. *634:*191–202.

Ross, C.A., D. Bredt, and S.H. Snyder (1990) Messenger molecules in the cerebellum. Trends Neurosci. *13:*216–222.

Ross, C.A., S.K. Danoff, M.J. Schell, S.H. Snyder, and A. Ullrich (1992) Three additional inositol 1,4,5-trisphosphate receptors: Molecular cloning and differential localization in brain and peripheral tissues. Proc. Natl. Acad. Sci. USA *89:*4265–4269.

Ryugo, D.K., and S.K. May (1993) The projections of intracellularly labeled auditory nerve fibers to the dorsal cochlear nucleus of cats. J. Comp. Neurol. *329:*20–35.

Sharp, A.H., T.M Dawson, C.A. Ross, M. Fotuhi, R.J. Mourney, and S.H. Snyder (1993a) Inositol 1,4,5-trisphosphate receptors: Immunohistochemical localization to discrete areas of rat central nervous system. Neuroscience *53:*927–942.

Sharp, A.H., P.S. McPherson, T.M. Dawson, C. Aoki, K.P. Campbell, and S.H. Snyder (1993b) Differential immunohistochemical localization of inositol 1,4,5-trisphosphate- and ryanodine-sensitive Ca^{2+} release channels in rat brain. J. Neurosci. *13:*3051–3063.

Suburo, A.M., J. Rodrigo, M.L. Rossi, R. Martínez-Murillo, G. Terenghi, N. Maeda, K. Mikoshiba, and J.M. Polak (1993) Immunohistochemical localization of the inositol 1,4,5-trisphosphate receptor in the human nervous system. Brain Res. *601:*193–202.

Sudhof, T.C., C.L. Newton, B.T. 3d, Y.A. Ushkaryov, and G.A. Mignery (1991) Structure of a novel InsP3 receptor. EMBO J. *10:*3199–3206.

Supattapone, S., P.F. Worley, J.M. Baraban, and S.H. Snyder (1988) Solubilization, purification, and characterization of an inositol trisphosphate receptor. J. Biol. Chem. *262:*741–745.

Tsuchitani, C. (1978) Lower auditory brain stem structures of the cat. In R.F. Naunton and C. Fernandez (eds): Evoked Electrical Activity in the Auditory Nervous System. New York, Academic Press, pp. 373–401.

Warr, W.B. (1982) Parallel ascending pathways from the cochlear nucleus. Contri. Sens. Physiol. *7:*1–38.

Worley, P.F., J.M. Baraban, and S.H. Snyder (1989) Inositol 1,4,5-trisphosphate receptor binding: autoradiographic localization in rat brain. J. Neurosci. *9:*339–346.

Wouterlood, F.G., and E. Mugnaini (1984) Cartwheel neurons of the dorsal cochlear nucleus. A Golgi–electron microscopic study in the rat. J. Comp. Neurol. *227:*136–157.

Wouterlood, F.G., E. Mugnaini, K.K. Osen, and A.-L. Dahl (1984) Stellate neurons in rat dorsal cochlear nucleus studied with combined Golgi impregnation and electron microscopy: Synaptic connections and mutual coupling by gap junctions. J. Neurocytol. *13:*639–664.

Wright, D.D., C.D. Blackstone, R.L. Huganir, and D.K. Ryugo (1993) Immunocytochemical localization of a metabotropic glutamate receptor (mGR1α) within the dorsal cochlear nucleus of the rat. Ass. Res. Otolaryngol. Abstr. *16:*122.

Young, E.D., W.P. Shofner, J.A. White, J.-M. Robert, and H.F. Voigt (1988) Response properties of cochlear nucleus neurons in relationship to physiological mechanisms. In G.M. Edelman, W.E. Gall, and W.M. Cowan (eds): Auditory Function: Neurobiological Bases of Hearing. New York: J. Wiley & Sons, pp. 277–312.

Zhang, S., and D. Oertel (1993) Cartwheel and superficial stellate cells of the dorsal cochlear nucleus of mice: Intracellular recordings in slices. J. Neurophysiol. *69:*1384–1397.